# Spatially Dependent Inelastic Tunneling in a Single Metallofullerene

M. Grobis,[1] K. H. Khoo,[1] R. Yamachika,[1] Xinghua Lu,[1] K. Nagaoka,[1,*] Steven G. Louie,[1] M. F. Crommie,[1] H. Kato,[2] and H. Shinohara[2]

[1]*Department of Physics, University of California at Berkeley, Berkeley, California 94720-7300, USA and Materials Sciences Division, Lawrence Berkeley Laboratory, Berkeley, California 94720-7300, USA*

[2]*Department of Chemistry & Institute for Advanced Research, Nagoya University, Nagoya 464-8602, Japan*

(Received 21 December 2004; published 6 April 2005)

We have measured the elastic and inelastic tunneling properties of isolated Gd@$C_{82}$ molecules on Ag(001) using cryogenic scanning tunneling spectroscopy. We find that the dominant inelastic channel is spatially well localized to a particular region of the molecule. *Ab initio* pseudopotential density-functional theory calculations indicate that this channel arises from a vibrational cage mode. We further show that the observed inelastic tunneling localization is explained by strong localization in the molecular electron-phonon coupling to this mode.

DOI: 10.1103/PhysRevLett.94.136802 PACS numbers: 73.63.-b, 63.22.+m, 68.37.Ef

Relentless miniaturization of electronic circuitry has motivated study into the possible use of single molecules as electronic components [1]. Endohedral fullerene molecules are exciting candidates for such nanotechnological applications due to their electronic and magnetic flexibility [2]. Molecular components, however, differ from conventional electronic elements in the degree to which mechanical degrees of freedom affect electrical conductivity [3,4]. Understanding this behavior in molecular systems is complicated by difficulties in identifying conductance-affecting molecular modes and by discrepancies between single molecule and ensemble measurements [5,6]. These discrepancies are not well understood, but have been speculated to arise from molecular electron-phonon coupling selection rules [7,8] and effects due to phonon dynamics, such as the orientation of phonon displacements with respect to tunneling electrodes [9].

In this Letter, we present a unified experimental and theoretical inelastic scanning tunneling spectroscopy (IESTS) study of a single endohedral fullerene molecule, aimed at understanding the role of local spatial variations in the electron-phonon coupling of this molecular system. We experimentally probed isolated Gd@$C_{82}$ molecules residing on Ag(001) and found signatures of several well-resolved elastic and inelastic conductance channels. The dominant inelastic signal is spatially localized and detectable only on certain parts of the Gd@$C_{82}$ molecule. Density-functional theory (DFT) calculations show that this inelastic signal can be explained by considering the coupling of molecular phonon modes to the molecular electronic state located at the Fermi level. Coupling to the inner Gd atom appears to be unimportant in our experimental regime. Though the molecular phonon modes and electronic wave function extend over the whole molecule, we show that the expected coupling of the dominant cage vibrational mode to the electronic molecular wave function is spatially localized, leading to highly localized IESTS signals. This suggests that differences between molecular layer and single molecule inelastic tunneling measurements might arise from the limited sampling of molecular locations in single molecule experiments [5,6].

Our experiments were conducted using a homebuilt ultrahigh vacuum (UHV) STM with a PtIr tip. The single-crystal Ag(001) substrate was cleaned in UHV, cooled to ~80 K, and then dosed with Gd@$C_{82}$ before being cooled to 7 K in the STM stage. $dI/dV$ spectra and images were measured through lock-in detection of the ac tunneling current driven by a 450 Hz, 1–10 mV (rms) signal added to the junction bias under open-loop conditions (bias voltage here is defined as the sample potential referenced to the tip). Over 50 Gd@$C_{82}$ molecules were examined in this study. We deposited an additional dilute coverage of $C_{60}$ as a reference molecule for determining the quality of the STM tip. All data were acquired at 7 K.

The topographic structure of two Gd@$C_{82}$ molecules residing next to a single $C_{60}$ molecule on Ag(001) is shown in the STM image in Fig. 1. Gd@$C_{82}$ molecules adsorb mainly to the bottoms of step edges and display two orientations (seen in Fig. 1) that differ by ~30° rotation about an axis parallel to the surface. Gd@$C_{82}$ shows pronounced internal structure when imaged with a bias of

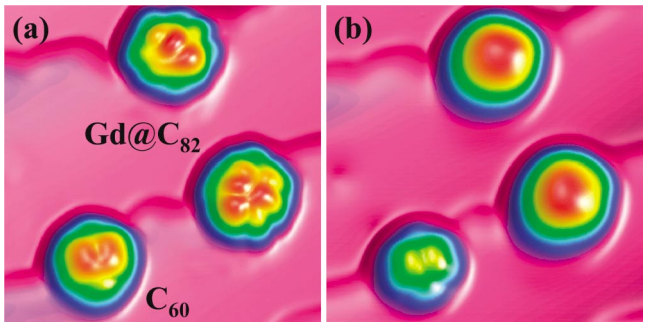


FIG. 1 (color). Constant current topographs (65 Å × 65 Å) of two Gd@$C_{82}$ molecules alongside a $C_{60}$ reference molecule taken at (a) 0.1 V, 1 nA and (b) 2.0 V, 1 nA.

 

0.1 V [Fig. 1(a)], but appears smooth and featureless when imaged at higher biases [Fig. 1(b), $V = 2.0$ V]. This is in contrast to the lobed structure of $C_{60}$ which does not show significant dependence on positive imaging bias.

The detailed spatial and energetic dependence of metallofullerene electronic wave functions was measured by performing differential conductance ($dI/dV$) spectroscopy and imaging on individual Gd@$C_{82}$ molecules. Figure 2 shows $dI/dV$ spectra acquired at different points on a single Gd@$C_{82}$ molecule (orientation shown in inset). The spectra reveal six molecular states, located at $-0.85$, 0.10, 0.65, 1.00, 1.32, 1.66 V ($\pm 0.05$ V). Each molecular state has a unique spatial dependence (shown in the energy-resolved $dI/dV$ images of Fig. 2) that differs substantially from the topographic structure seen in Fig. 1. These results differ from previous scanning tunneling spectroscopy (STS) measurements on endohedral molecules in that the regions of high spectral density ("bright spots") vary spatially with energy and cannot be conclusively linked with the interior atom location [10,11]. We find that Gd@$C_{82}$ $dI/dV$ spectra and spatial maps are sensitive to STM tip termination. Reproducible images and spectroscopic results were achieved only with tips that gave undistorted images and spectra when tested on nearby $C_{60}$ reference molecules [12].

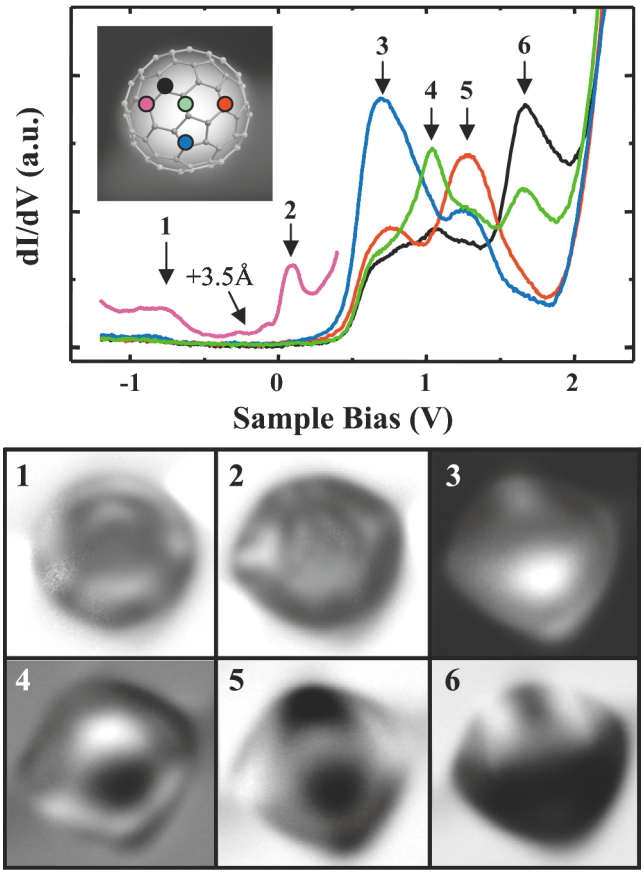


FIG. 2 (color). $dI/dV$ spectra taken at different points on a single Gd@$C_{82}$ molecule (points shown in inset). Inset shows a constant current topograph (35 Å × 35 Å) of Gd@$C_{82}$ overlaid with the best fit $C_{82}$ cage orientation. (1)–(6) Energy-resolved spectral maps (35 Å × 35 Å) of molecular resonances seen at (1) $-0.85$ V, (2) 0.10 V, (3) 0.65 V, (4) 1.00 V, (5) 1.32 V, and (6) 1.66 V, respectively. Tip stabilization parameters: $V = 2.0$ V and $I = 0.3$ nA. The pink spectrum (marked +3.5 Å) and spectral maps (1) and (2) were acquired after bringing the tip 3.5 Å closer to the molecule.

Vibrational excitations of individual Gd@$C_{82}$ molecules were examined by measuring $d^2I/dV^2$ spectra at low bias ($dI/dV$ spectra were numerically differentiated). Clear inelastic tunneling channels were observed as pairs of antisymmetric peaks in $d^2I/dV^2$, as seen in Fig. 3. The three main inelastic channels observed correspond to excitations of 43, 60, and 70 mV ($\pm 1$ mV). These modes lead to total increases in differential conductance of approximately 5, 15, and 2%, respectively (for positive bias). $d^2I/dV^2$ spectra taken on the bare Ag(001) as a reference [red curve in Fig. 3(a)] do not show these inelastic channels.

The Gd@$C_{82}$ inelastic signal shows strong spatial inhomogeneity over the surface of an individual molecule and is detectable only in a localized region. This can be seen in Fig. 3(b), which shows an image of $d^2I/dV^2$ mapped across a single Gd@$C_{82}$ molecule for the dominant 60 mV mode (molecular orientation here is the same

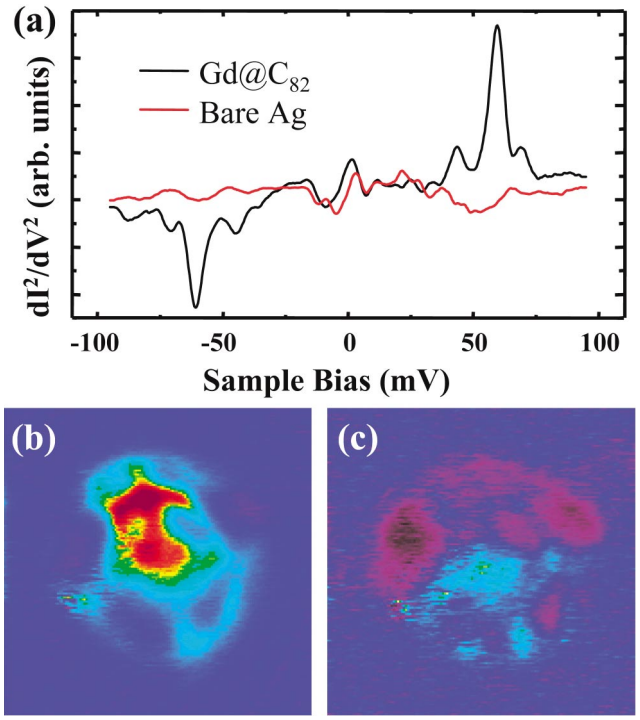


FIG. 3 (color). (a) $d^2I/dV^2$ spectra taken at a single point in the upper part of the Gd@$C_{82}$ molecule shown in Fig. 2 (black line) and on the bare Ag(001) surface (red line). (b) Spatial map (35 Å × 35 Å) of the $d^2I/dV^2$ inelastic signal at 60 mV. (c) Spatial map of the $d^2I/dV^2$ reference signal at 80 mV.

as in Fig. 2). An off-resonance $d^2I/dV^2$ image of the molecule taken at 80 mV [Fig. 3(c)] does not show any significant features, indicating that extraneous image contributions (such as tip trajectory and energy dependent changes in electronic structure [12,13]) do not play a strong role in the on-resonance image at 60 mV.

It is surprising that the main Gd@$C_{82}$ vibrational mode produces such a spatially localized IESTS signal, given that molecular vibrations tend to have a more delocalized nature. IESTS images of simpler molecules, such as acetylene [14] and oxygen [15], typically reflect the spatial extent of the measured vibrational modes. In order to understand the localized behavior seen here, we first consider how the inelastic tunneling signal arises from the electronic and vibrational properties of a single Gd@$C_{82}$ molecule. A molecular phonon affects electronic conductance near the Fermi level ($E_F$) if it couples electronic states at $E_F + \hbar\omega$ to states at $E_F$, where $\hbar\omega$ is the phonon energy. The magnitude of the resulting change in $dI/dV$ can be estimated using Fermi's Golden Rule:

$$\Delta dI/dV|_{eV=\hbar\omega} \sim |\langle\psi_{E_F}|V_{\text{el-ph}}|\psi_{E_F+\hbar\omega}\rangle|^2. \quad (1)$$

Here, $V_{\text{el-ph}}$ is the electron-phonon coupling term for molecular phonons: $V_{\text{el-ph}} = \sum_i \frac{dH_e}{dQ_i}|_{Q_i=0}\Delta Q_i$, where $H_e$ is the molecular electronic Hamiltonian and $\Delta Q_i$ is the displacement of the $i$th atom along the canonical phonon coordinate (with the normalization $\sum_i m_i(\Delta Q_i)^2 = \frac{\hbar}{2\omega}$) [8]. In the quasi-static limit ($\hbar\omega \to 0$) the average IESTS signal can be written as

$$\Delta dI/dV|_{eV=\hbar\omega} \sim \left|\sum_i \frac{dE_{\psi_{E_F}}}{dQ_i}\frac{1}{\sqrt{\omega}}\right|^2. \quad (2)$$

Spatial characteristics of the IESTS signal can be computed by considering a two-step tunneling process where electrons are first elastically injected at the position $\mathbf{r}_0$ into a molecular state of energy $E_F + \hbar\omega$, and then transition inelastically to states at $E_F$. The spatially dependent rate of this process can be derived via second order Fermi's Golden Rule to give [7]

$$\Delta dI/dV|_{eV=\hbar\omega}(r_0) \sim \left|\sum_i \left\langle\frac{d\psi_{E_F}}{dQ_i}|r_0\right\rangle\frac{1}{\sqrt{\omega}}\right|^2. \quad (3)$$

To address the origin of inelastic signals observed here for a single Gd@$C_{82}$ metallofullerene molecule, we used an *ab initio* density-functional method [16] to evaluate Eqs. (2) and (3). The details of our calculation method are described in Ref. [17]. For simplicity, we performed our calculations on a bare $C_{82}$ cage with no interior Gd atom. Neglecting the inner Gd atom is justified by noting that (1) electronic cage states near $E_F$ are only weakly perturbed by the inner atom [18] and (2) our observed vibrational energies are in the range of $C_{82}$ cage, and not inner atom, phonon energies, indicating $C_{82}$ phonons are responsible for the inelastic signal [19]. Hence, the presence of the Gd atom should be only a small perturbation on the dynamics dictated by Eqs. (2) and (3) in our energy range. Charge transfer to the $C_{82}$ cage from the Gd atom and substrate was treated as a single fitting parameter. The best theoretical fits were obtained for a molecular charge state of $-4$. This was determined by comparison of STS spectra, $dI/dV$ images, and electronic state symmetries [20]. The $-4$ charge state is reasonable since Gd is known to donate three electrons to the $C_{82}$ cage [21] and Ag substrates are expected to donate charge to fullerenes [17]. The $C_{82}$ cage orientation, seen in the inset in Fig. 2, was deduced by comparing experimental and theoretical $dI/dV$ maps. In this orientation, the Gd atom is located near the molecule-Ag(001) interface [21].

The resulting theoretical phonon spectrum for an isolated $C_{82}$ cage is shown in Fig. 4(a), with each vibrational mode shown as a black vertical line. The theoretical inelastic tunneling spectrum (red lines) was obtained by calculating the electron-phonon coupling of each molecu-

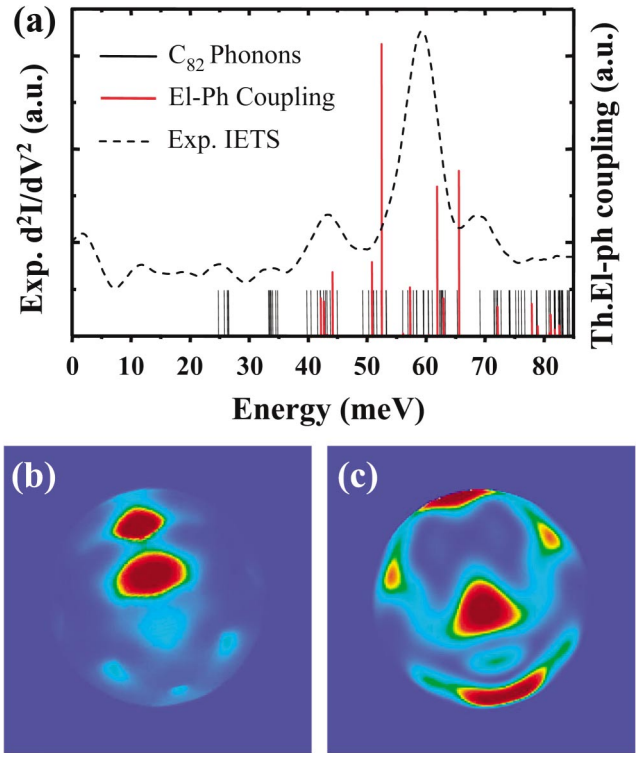


FIG. 4 (color). (a) Theoretical vibrational spectrum for an isolated $C_{82}$ molecule charged with four electrons is shown as black vertical lines. Red vertical lines show the electron-phonon coupling between each phonon mode and the $C_{82}$ electronic state at $E_F$. The dotted curve is the experimental inelastic tunneling signal. (b) Simulated inelastic tunneling map for the dominant phonon mode at 52 mV (c) Spatial map of the magnitude of the bare atomic displacements of the dominant phonon mode (broadened by 1.0 Å). The color scales used in Figs. 3 and 4 are identical and represent standard deviations of the measured or computed on-molecule signal above the off-molecule background.

lar vibrational mode to the $C_{82}$ electronic cage state at $E_F$ [via Eq. (2)]. Of the 90 vibrational modes in this energy window, only a few show appreciable coupling to the $C_{82}$ cage state at $E_F$. The relative electron-phonon coupling of these modes is in reasonable agreement with the experimental $d^2I/dV^2$ spectrum and indicates that the cage mode with the theoretical energy of 52 meV is responsible for the dominant experimental inelastic tunneling channel. In order to understand the spatial localization of our inelastic signal, we calculated the spatial dependence of the electron-phonon coupling for this mode using Eq. (3) [22]. The resulting theoretical map [Fig. 4(b)] shows a striking localization of the IESTS signal in the upper half of the molecule, in good agreement with the experimental observation [Fig. 3(b)]. The small deviation between calculated and theoretical phonon energies is likely due to effects of the substrate [23] and inner atom [24], which we ignored in our calculation. The general level of agreement, however, suggests that these effects play only a small role in the qualitative behavior of electron-phonon coupling in $Gd@C_{82}$, beyond determining the cage charge state.

Our calculation allows us to explicitly compare the spatial dependence of the molecular electron-phonon coupling (i.e., the source of the IESTS signal) with the spatial distribution of atomic displacement magnitudes for the corresponding cage phonon mode [Fig. 4(b) vs Fig. 4(c)]. It is interesting to note that areas of high atomic phonon displacement are nearly anticorrelated with the inelastic tunneling maxima. This behavior stems from the fact that inelastic tunneling is determined by the *rate* electronic wave functions are deformed by phonon displacements, as dictated by Eq. (3). Maximums in $d\Psi/dQ$ need not be correlated with maximums in $\Psi$ or $Q$, and this interplay between electron wave functions and phonon dynamics can produce a surprising localization in the inelastic tunneling, as seen in our study. The emergence of such localization might explain the increase in the number of vibrational modes detected in molecular film measurements compared to IESTS measurements. Molecular films contain a large number of molecular configurations and thus are more likely to sample areas of highly localized electron-phonon coupling in comparison to an STM tip.

In conclusion, we have observed strong inelastic tunneling into single metallofullerene molecules via STS. Spatial mapping of the dominant inelastic channel shows that it is highly localized to a small area of the molecule's surface. Comparison of local spectroscopy with DFT calculations indicates that this channel arises from a vibrational cage mode and is not strongly influenced by the interior ion. Spatial localization in the IESTS signal is explained by strong spatial localization in the molecular electron-phonon coupling to this mode and shows no correlation with the spatial extent of the mode itself. This work suggests that limited spatial sampling can significantly influence the number of channels detected via inelastic tunneling.

This work was supported in part by NSF Grants No. DMR04-39768 and No. EIA-0205641 and by the Director, Office of Energy Research, Office of Basic Energy Science, Division of Material Sciences and Engineering, U.S. Department of Energy under Contract No. DE-AC03-76SF0098. Computational resources have been provided by DOE at the National Energy Research Scientific Computing Center.

*Present address: Nanomaterial Laboratory, National Institute for Materials Science, Tsukuba 305-0044, Japan.

[1] J. R. Heath and M. A. Ratner, Phys. Today **56**, No. 5, 43 (2003).
[2] H. Shinohara, Rep. Prog. Phys. **63**, 843 (2000).
[3] *Tunneling Spectroscopy*, edited by P. K. Hansma (Plenum, New York, 1982).
[4] B. C. Stipe, M. A. Rezaei, and W. Ho, Science **280**, 1732 (1998); H. Park *et al.*, Nature (London) **407**, 57 (2000).
[5] S. Nolen and S. T. Ruggiero, Chem. Phys. Lett. **300**, 656 (1999).
[6] J. I. Pascual *et al.*, J. Chem. Phys. **117**, 9531 (2002).
[7] N. Lorente and M. Persson, Phys. Rev. Lett. **85**, 2997 (2000).
[8] N. Mingo and K. Makoshi, Phys. Rev. Lett. **84**, 3694 (2000); N. Lorente *et al.*, Phys. Rev. Lett. **86**, 2593 (2001).
[9] J. Kirtley, D. J. Scalapino, and P. K. Hansma, Phys. Rev. B **14**, 3177 (1976).
[10] A. Taninaka *et al.*, Nano Lett. **3**, 337 (2003); R. Klingeler *et al.*, Surf. Sci. **553**, 95 (2004).
[11] K. Wang *et al.*, Phys. Rev. Lett. **91**, 185504 (2003).
[12] X. Lu *et al.*, Phys. Rev. Lett. **90**, 096802 (2003).
[13] M. Grobis *et al.*, *Proceedings of the Twelfth International Conference STM/STS*, AIP Conf. Proc. No. 696 (AIP, New York, 2003), p. 20.
[14] B. C. Stipe, M. A. Rezaei, and W. Ho, Phys. Rev. Lett. **82**, 1724 (1999).
[15] J. R. Hahn, H. J. Lee, and W. Ho, Phys. Rev. Lett. **85**, 1914 (2000).
[16] W. Kohn, L. J. Sham, Phys. Rev. **140**, A1133 (1965); H. J. Choi, M. L. Cohen, S. G. Louie, Physica C (Amsterdam) **385**, 66 (2003).
[17] X. Lu *et al.*, Phys. Rev. B **70**, 115418 (2004).
[18] J. Lu, X. Zhang, X. Zhao, S. Nagase, and K. Kobayashi, Chem. Phys. Lett. **332**, 219 (2000); L. Senapati, J. Schrier, and K. B. Whaley, Nano Lett. **4**, 2073 (2004).
[19] M. Krause, P. Kuran, U. Kirbach, and L. Dunsch, Carbon **37**, 113 (1999).
[20] The actual charge state in our calculation was $-4.01$. The extra charge determined which molecular state aligned with $E_F$.
[21] E. Nishibori *et al.*, Phys. Rev. B **69**, 113412 (2004).
[22] The calculation was performed over a simulated constant current surface as in Ref. [12].
[23] J. Kirtley and P. K. Hansma, Phys. Rev. B **13**, 2910 (1976).
[24] B. Kessler *et al.*, Phys. Rev. Lett. **79**, 2289 (1997).